JOURNAL OF PETROLEUM GEOMECHANICS
(JPG)

Original article

Oil-contamination impact on bearing capacity of strip footing placed on geocell-reinforced sand under eccentric load

Mohammad Samed Jahanian[1], Arash Razmkhah[1*], Hasan Ghasemzadeh[2], Hamidreza Vosoughifar[1]

1- Department of Civil Engineering, South Tehran Branch, Islamic Azad University, Tehran, Iran
2- Civil Engineering Faculty, K. N. Toosi University of Technology, Tehran, Iran

Received: 23 September 2023; Accepted: 24 October 2023

DOI: 10.22107/JPG.2023.417661.1210

Keywords

Bearing capacity,
Strip footing,
Geocell,
Sand,
Eccentricity,
Oil-contaminated

Abstract

The infiltration of crude oil and its derivatives into the soil leads to changes in the mechanical behavior of the soil in addition to detrimental and environmental problems. This study aims to evaluate the bearing capacity of geocell-reinforced strip footings laid on oil-contaminated sand under eccentric load via numerical modeling using PLAXIS 2D. The behavior of the footing is assessed regarding various oil contents of 0, 3, 6, 9, and 12% under loading with different eccentricities of e/B=0, 1/12, 1/6, and 1/3. Numerical results revealed that soil pollution has a negative effect on the performance of strip footings, so that an increase in oil content led to a reduction in the magnitude of the load capacity. It was observed that reinforcement with geocell increases the bearing capacity of footing located on the oil-contaminated medium under different eccentricities. The effect of reinforcing with geocell was higher for contaminated soil compared to clean one. Further, the load capacity improvement factor (IF) increased by increasing oil content and settlement value. The results revealed that the reinforcing effect increased with an increase in load eccentricity for both clean and contaminated soils. In addition, the use of geocells is most effective when the loading is outside the core of the foundation, i.e., e/B>1/6. The footing tilting around the centerline axis of the footing due to load eccentricity as well as soil reinforcement with geocell led to a reduction in the stress-affected zone and as a result the displacement depth of the soil beneath the foundation.

1. Introduction

The bearing capacity estimation of surface footings using various methods has always been an essential issue in soil mechanics and foundation engineering [1-2]. Evaluating the actual parameters of the bed soils is vital for foundation design. Soil contaminated with oil is among the problematic soils. Several studies have raised our understanding of the oil pollution's effect on the physical and mechanical properties of the soil [3-7]. One of the appropriate and economical methods to solve the problem of contaminated soil is to use these soils in construction projects [8]. The results reported by Khamehchiyan et al. [9] demonstrated that the oil contamination of the soils causes a decrease in strength, permeability, and dry unit weight. Karkush and Kareem [10] showed that soil contamination with 10 and 20% of fuel oil leads to a decrease in cohesion by about 44 and 67%, respectively; whereas, the reduction of internal friction angle was 20 and 32%, respectively. Obviously, with the change in geotechnical parameters due to the presence of oil, the foundation design parameters will change. Nasr [11] revealed that the ultimate bearing capacity of the soil is extremely reduced in oil-contaminated sands. The results reported by Hosseini and Boushehrian [12] showed that contamination of the soil with diesel fuel and kerosene could affect the final settlement and the number of loading cycles required to achieve this settlement. Joukar

*** Corresponding Author:** Iran, Tehran, Islamic Azad University, South Tehran Branch, Department of Civil Engineering, Tel: 09121447223, Email: a_razmkhah@azad.ac.ir.

and Boushehrian [13] indicated that increasing the pollutant content in the sand and the depth of contamination leads to a reduction in the bearing capacity. Indeed, the failure mechanism of the soil changes due to the presence of pollutants within the soil and reduces the carrying capacity [14]. Shin et al. [15] showed that increasing the oil content to 1.3% reduces the bearing capacity by about 75%. Nasr [16] showed that the coefficient N_γ should be reduced based on the type and percentage of the contaminated oil. As can be discerned, the oil content has a remarkable effect on the strength parameters of the soil, and it should be considered for foundation design purposes.

The beneficial effects of geocells to increase the bearing capacity have been demonstrated by several researchers [17-26]. The stresses and strains under the foundation are reduced by transferring the load to the deeper layers using the geocell layer [27]. Dash et al. [28] reported that geocell cells prevent lateral deformation by soil confinement, resulting in a rigid composite beneath the footing, which increases the load capacity. By increasing the width of the geocell layer and increasing the number of cells, the resistance to lateral movement increases [29]. Decreasing the aperture size of the cell wall caused more soil confinement and thus improved the footing performance [30]. The positive effect of geocell depends on the grain size of the soil so that an increase in the bearing capacity caused by the geocell is more visible for coarse aggregates [31]. Mehrjardi et al. [32] recommended that the size of the geocell cells should be smaller than 0.67 times the footing's width. Findings revealed that the load capacity of geocell-reinforced soil is enhanced with an increase in the tensile strength of geocell materials [33]. Thus, the geometric features of the geocell play an important role in the behavior of reinforced soil.

Many studies have considered the planar reinforcers to reinforce the soil beneath the footings, both under central and with eccentric loads [34-38]. Furthermore, the performance of geocells in strengthening the bed soil has been investigated under loading exerted along the centerline of the footing [39-41]. However, the effect of load eccentricity on surface foundations laid on sand reinforced with geocell has not been considered. Several studies have evaluated the performance of geocells using numerical methods. However, numerically modeling the geocell is not easy due to the honeycomb structure of the reinforcer. In some numerical modeling, the geocell-soil composite layer is considered a soil layer with modified resistance parameters [42-44]. Hegde and Sitharam [45] examined the effect of cell opening size as a variable parameter on bearing capacity by numerical simulation using FLAC 3D. Chowdhury and Patra [46] evaluated the effect of geocell on the settlement behavior of circular footing under combined static and cyclic loadings using PLAXIS 2D. Numerical modeling has been performed for soils reinforced with geocell. However, no study has been reported on geocell-reinforced soil under eccentric loading considering oil pollution.

In the present study, finite element analysis was performed using PLAXIS 2D to investigate the behavior of geocell-reinforced strip footings under static eccentric loadings with and without oil pollution. The results of the numerical modeling were compared with those obtained from experimental tests. The behavior of strip footing laid on clean sand was evaluated under different load eccentricities; thereafter, it was examined for oil-contaminated sand models and it was compared with the non-contaminated soil conditions.

2. Test materials and elements of the model

The Mohr-Coulomb criterion, which is an elastic-plastic criterion and the most popular model to characterize the shear failure of the soil, was used to predict the behavior of the bed soil. This model can accurately identify the failure plane that occurs in a plane with critical normal and shear stresses, and it is defined as follows:

$$\tau = c + \sigma . tan(\varphi) \quad (1)$$

In which τ is the shear stress, c is the soil's cohesion, σ is the normal stress, and φ is the internal friction angle of the soil. According to the relations in the Mohr circle, the following relations can be derived:

$$\sigma = \sigma_m - \tau_m . \sin(\varphi) \quad (2)$$

$$\tau = \tau_m . \cos(\varphi) \quad (3)$$

In which $\sigma_m=(\sigma_1+\sigma_3)/2$ is the mean normal stress and $\tau_m=(\sigma_1-\sigma_3)/2$ is the mean shear stress. Note that σ_1 and σ_3 are the maximum and minimum principal stresses, respectively. Table 1 provides a list of the sand's mechanical properties. A strip footing on a sand layer is modeled with a 25 mm thick steel plate. The footing dimensions are 39.8

and 1 cm in width and length, respectively. Note that the length of the foundation is considered a unit in the plane strain conditions.

Table 1. Mechanical Properties of the soil

Property	Value
Unit weight (kN/m^3)	15
Poisson ratio	0.3
Cohesion (kPa)	3.25
Friction angle (degree)	34
Dilatation angle (degree)	4
Young's module (kPa)	6.5*10^3

The equivalent composite approach has been applied in this study for the numerical modeling of geocell layers. The geocell's cellular structure, which is impossible to represent in two dimensions, is the key cause of this problem. In other words, the sand-filled geocell layer can be regarded as a soil layer with modified resistance. In this case, the friction angle and specific weight of the composite are considered equivalent to the friction angle and unit weight of the subgrade soil, based on prior findings [47-48]. However, because of the confinement feature of the geocell, the corresponding composite will have a greater cohesion than the subsoil [49]. According to the findings of the latter study, Eq. (4) can be used to determine the cohesion value caused by the geocell (c_r):

$$c_r = \frac{\Delta\sigma_3}{2}\sqrt{k_p} \quad (4)$$

In which k_p is the passive soil pressure coefficient and $\Delta\sigma_3$ is the additional confining pressure generated by membrane stresses. Eq. (5) can be utilized to calculate $\Delta\sigma_3$ value:

$$\Delta\sigma_3 = \frac{2M}{d_g}\left(\frac{1-\sqrt{1-\varepsilon_a}}{1-\varepsilon_a}\right) \quad (5)$$

Where d_g and M are the diameter of the equivalent circular area of the geocell's pocket size and the tensile strength of the geocell material in the axial strain ε_a, respectively.

According to the geocell layer utilized in the study by Jahanian et al. [50], the value of dg is equal to 5.7 cm. Additionally, tensile strength 70 kN/m was computed for 5% axial strain. Eqs. (4) and (5) can therefore be applied to calculate the cohesion value of the geocell layer, which was 62 kPa. Madhavi Latha [51] showed that the elastic modulus (E_g) of the sand-filled geocell layer can be obtained as follows:

$$E_g = 4(\Delta\sigma_3)^{0.7}(k_u + 200M^{0.16}) \quad (6)$$

Where K_u is the unreinforced sand's dimensionless modulus value. The equivalent composite elastic modulus for K_u=240 was 47500 kPa.

The finite element model of the strip footing placed on geocell-reinforced sand under eccentric load (h/B=0.45, b/B=4, u/B=0.1) is depicted in Fig. 1. According to the findings of earlier research using an equivalent composite approach, it was not useful to employ the tensile capacity of a geocell layer filled with sand for horizontal ground cases. However, in the computational model of the strip footing where the load is applied along the centerline of the footing, the equivalent composite must be able to bear tensile stresses. Therefore, a layer of geogrid was put in the center of the composite at a certain height (H) from the footing base. The H values were chosen as 0.045, 0.04, 0.04, and 0.035 for e/B=0, 1/12, 1/6, and 1/3, respectively.

Oil-contaminated soil has different geomechanical features than uncontaminated soil. Based on the specified behavioral model, the cohesion and internal friction angle of the soil are essential properties. The effect of oil on sand can be disregarded since it has no impact on soil cohesion because sand has a cohesion value that is almost zero. Nasr [11] also reported similar results. Accordingly, it is believed that the cohesion of oil-contaminated sand is equivalent to that of clean sand. Based on the previous studies, the reduction of the internal friction angle of contaminated sand with soil contents of 3, 6, 9, and 12% was 32, 30, 28.5, and 27.5 degrees, respectively [11, 52]. Data from the study conducted by Soltani-Jigheh et al. [52] showed that the oil's viscosity, density (at 25◦C), American Petroleum Institute (API) gravity (at 60◦F), flash point, and specific gravity (at 25◦C) were equal to 41.2 g/ms, 0.895 g/cm3, 26.8, and 44.2 g/cm3, respectively.

As can be seen from Fig. 1, the interactions of the equivalent composite and geogrid with the soil and each other were both defined using the interface element. This interface was designated as a fully bonded interface for both contact modes (the resistance reduction factor, the Rinter=1.0). It should be noted that the boundary conditions for displacements were taken into account for all models. The model's bottom is constrained horizontally and vertically. The vertical boundaries are free to move in the vertical direction and restricted in the horizontal direction.

3. Meshing and numerical modeling

Fig. 2 displays the numerical model's meshing and boundary conditions. The physical model created by Jahanian et al. [50] and the numerical model considered in the current research completely match each other. To ensure that the displacement rises consistently until it reaches a specified maximum value, the loading is applied to the footing under displacement control conditions.

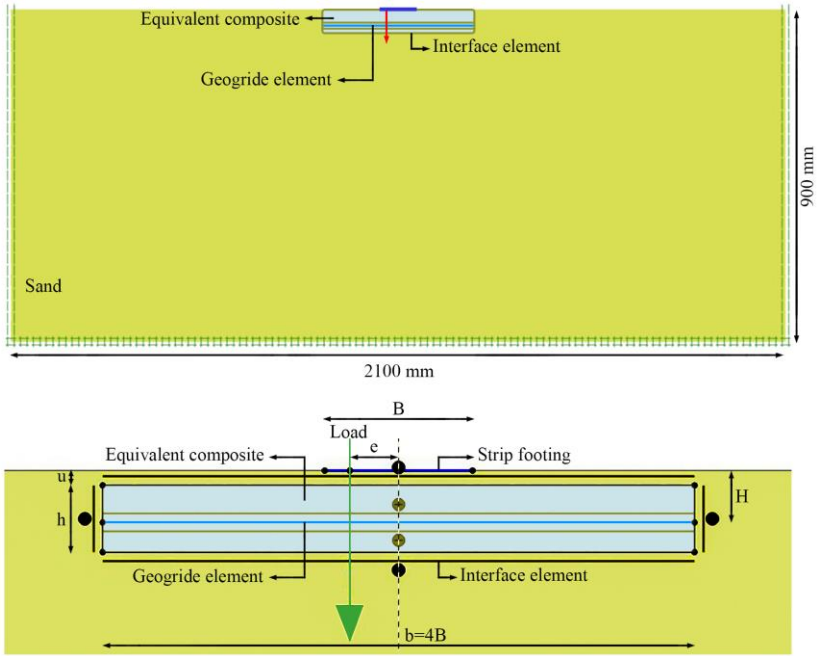

Fig. 1. Elements of the model including strip footing, soil, equivalent composite, and geogrid element

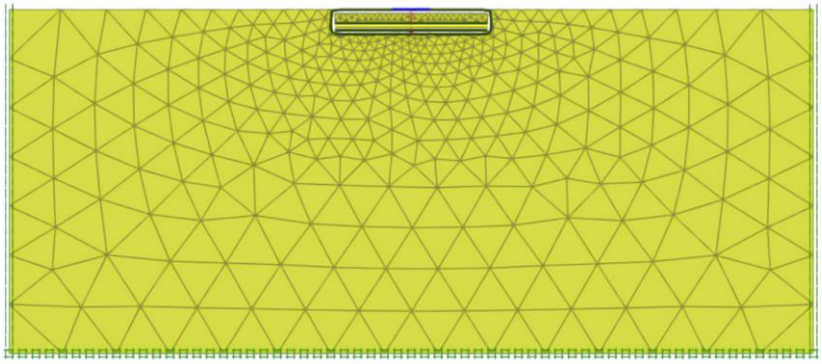

Fig. 2. Generated mesh and boundary conditions of the model

For the computational modeling of strip footings placed on unreinforced and geocell-reinforced sands exposed to eccentric load under plane strain conditions, the finite element program 2D Plaxis was employed. The simulated soil bed's dimensions match those of the physical model previously considered by Jahanian et al. [50], supporting the numerical models. Thus, the bed soil's width, length, and height were selected 0.4, 2.1, and 0.9 meters, respectively. The fixed parameters are the width of the footing (B), the height of the geocell (h), the length of the geocell (b), and the depth of the geocell's first layer (u), all of which are equal to 10, 1.0, 4.5, and 40 cm, respectively. The findings of the research conducted by Jahanian et al. [50] have been used to determine the constant values of u, h, and b. The oil content and load eccentricity (e) are two of the variable parameters. The oil contents were selected 0, 3, 6, and 12%. Because the load

eccentricity is considered in its non-dimensional form, the e/B ratio was chosen to be 0, 1/12, 1/6, and 1/3. It should be noted that the footing slides during loading were regarded in the laboratory models as a result of settlement and the rotation of the footing. Physical models that have the footing slide lead to an increase in eccentricity up to about 2 mm. As a result, the loading for the high and low eccentricities is increased by around 0.7 to 2 mm to match the eccentricity in numerical models with the actual eccentricity in the laboratory model. The reason for choosing this range is that the greater the eccentricity magnitude, the lower the settlement and sliding of the footing during failure. Accordingly, the value added to the eccentricity in the numerical model will be smaller. The depth of the geocell's first layer and also the height and length of the geocell are considered in the dimensionless forms of u/B=0.1, h/B=0.45, and b/B=4.0, respectively. The bearing capacity and the settlement values of footing are evaluated under different soil contents and load eccentricities. The set of numerical models performed in this study is presented in Table 2.

Table 2. Numerical tests program for the strip footings situated on the unreinforced and geocell-reinforced soils

Test Number	Type of reinforcement	Oil content (%)	e/B	H (m)
1, 2, 3, 4	unreinforced	0	0, 1/12, 1/6, 1/3	-
5, 6, 7, 8	unreinforced	3	0, 1/12, 1/6, 1/3	-
9, 10, 11, 12	unreinforced	6	0, 1/12, 1/6, 1/3	-
13, 14, 15, 16	unreinforced	9	0, 1/12, 1/6, 1/3	-
17, 18, 19, 20	unreinforced	12	0, 1/12, 1/6, 1/3	-
21	geocell reinforced	0	0	0.045
22	geocell reinforced	0	1/12	0.04
23	geocell reinforced	0	1/6	0.04
24	geocell reinforced	0	1/3	0.035
25	geocell reinforced	3	0	0.045
26	geocell reinforced	3	1/12	0.04
27	geocell reinforced	3	1/6	0.04
28	geocell reinforced	3	1/3	0.035
29	geocell reinforced	6	0	0.045
30	geocell reinforced	6	1/12	0.04
31	geocell reinforced	6	1/6	0.04
32	geocell reinforced	6	1/3	0.035
33	geocell reinforced	9	0	0.045
34	geocell reinforced	9	1/12	0.04
35	geocell reinforced	9	1/6	0.04
36	geocell reinforced	9	1/3	0.035
37	geocell reinforced	12	0	0.045
38	geocell reinforced	12	1/12	0.04
39	geocell reinforced	12	1/6	0.04
40	geocell reinforced	12	1/3	0.035

4. Numerical Verification

In Fig. 3, the bearing capacity of the strip footings laid on the unreinforced sand exposed to various eccentric loads using numerical modeling is compared to those derived from the laboratory models [50]. As can be observed, there is a favorable agreement between the numerical and laboratory results. The consistency reduces as the loading eccentricity increases. The comparison of geocell-reinforced sand for the case with h/B=0.45, b/B=4, and u/B=0.1 under different eccentricities is shown in Fig. 4. It is evident that the results also have a strong agreement with the reinforced cases. As can be discerned, the discrepancy between numerical and laboratory results for loading eccentricities of e/B=1/12 and 1/6 is negligible. In general, it can be stated that the methods of numerical modeling and experimental tests are in good agreement with each other in all cases.

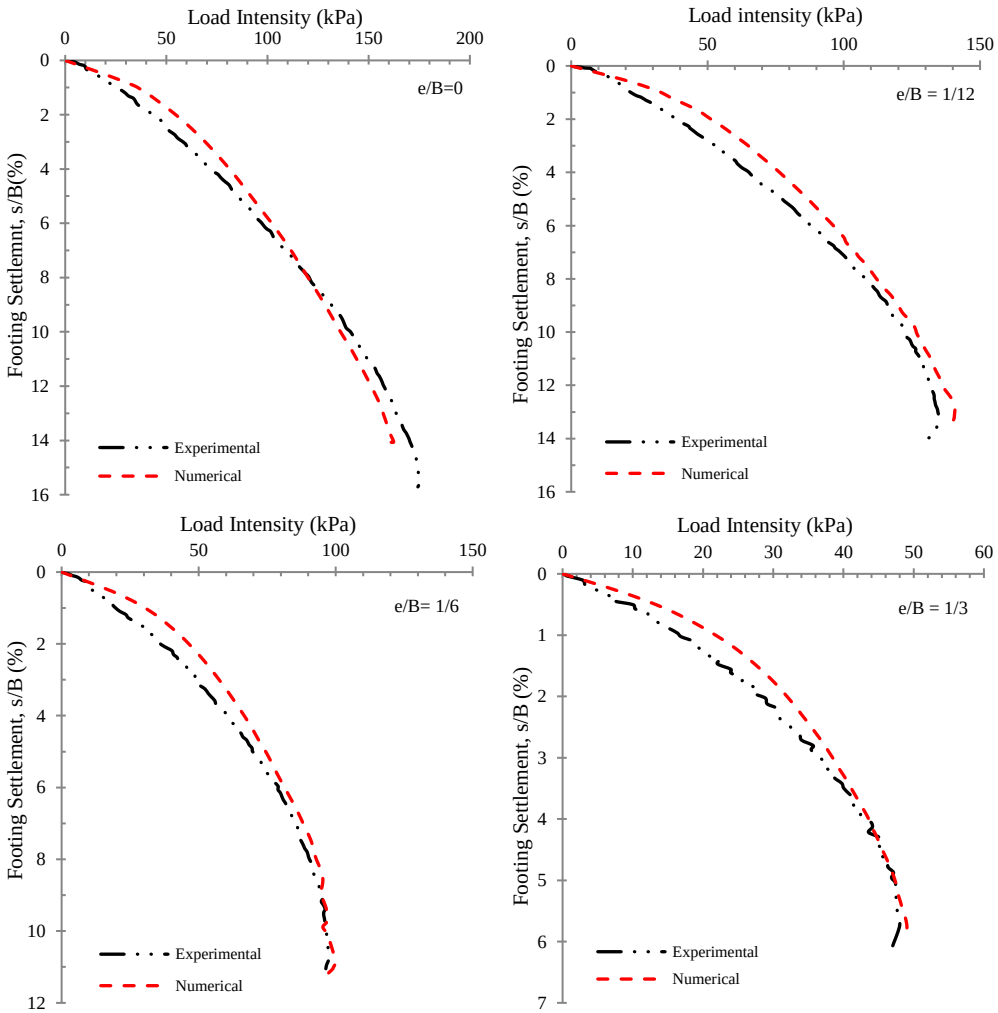

Fig. 3. Comparison of the bearing capacity for unreinforced conditions between numerical and experimental models

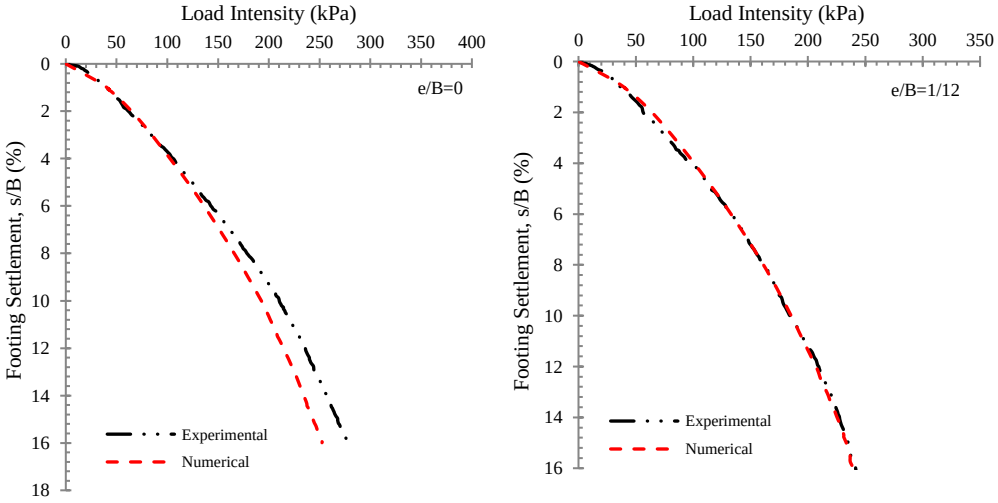

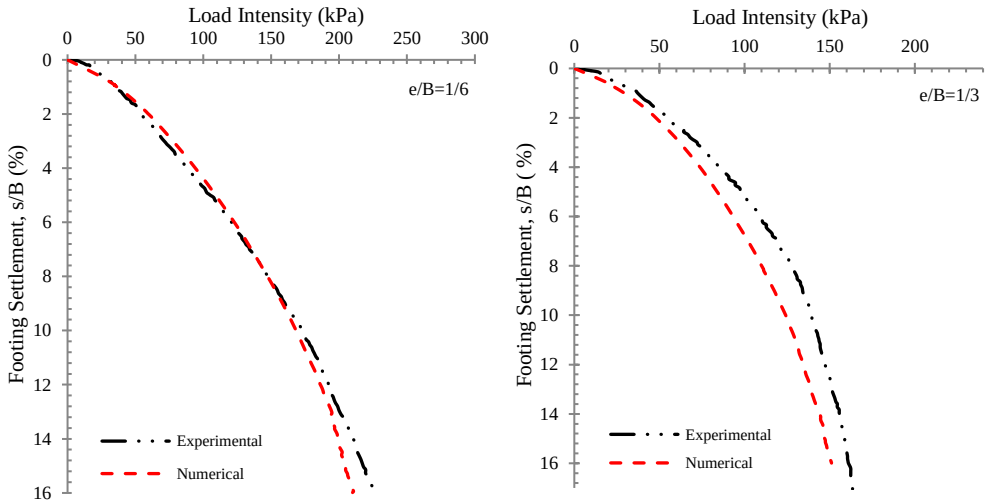

Fig. 4. Comparison of the bearing capacity for reinforced conditions between numerical and experimental models for b/B=4, h/B=0.45, u/B = 0.1

5. Results and Discussion

In this research, the increase in bearing capacity resulting from strengthening the bed soil with geocell has been shown using a dimensionless factor called the bearing capacity improvement factor (IF). This factor is defined as the ratio of the bearing capacity of the footing based on geocell-reinforced soil (q_g) at a certain settlement to the bearing capacity of the footing based on unreinforced soil (q) at the same settlement value under a similar eccentric loading. When this ratio is calculated at settlements beyond the ultimate bearing capacity of unreinforced soil, the ultimate bearing capacity of the foundation (q_{ult}) is used instead of q. Thus, it can be defined as follows:

$$IF_g = \frac{q_g}{q} \quad (7)$$

In most of the past research, the bearing capacity of geocell-reinforced foundations has been investigated at high and unrealistic settlements such as values up to 50% of the foundation's width [17, 28], while the large settlement values are not acceptable for designing of surface footings. Therefore, the bearing capacity improvement factor (IF) under loading with different eccentricities is considered for settlements equal to and less than 10% of the footing's width.

5.1 Bearing capacity of strip footing located on unreinforced clean sand

The load-settlement curves for unreinforced sands under loading with different eccentricities are shown in Fig. 5. As can be observed, the ultimate bearing capacity of unreinforced sand dramatically decreases with an increase in load eccentricity. The load capacity of unreinforced sand models for s/B ratios equal to 2, 5, and 10% is presented in Table 3. It can be seen that the ultimate bearing capacity for footings under loading with ratios of e/B=1/12, 1/6, and 1/3 is reduced by about 13, 41, and 70%, respectively. However, the reduction values under loading with the same eccentricities for settlement ratios of s/B=2.5 and 5% were equal to 6, 16, 43%, and 6, 19, 49%, respectively. This value for s/B=10% under loading eccentricity of e/B=1/12 was 7. It was observed that the soil failed for e/B=1/3 and 1/6. Thus, it can be concluded that the reduction rate of the load capacity significantly rises for e/B=1/3. Jahanian et al. [50] demonstrated that the reduction rate of the bearing capacity is higher when the load is exerted outside the core's footing, i.e. e/B>1.6. The findings of the previous studies carried out by Badakhshan and Noorzad [53] also showed similar results for square and circular footings and Gill and Mittal [54] for strip foundations located on the sand reinforced with rubber crumb.

5.2 The effect of oil content on the bearing capacity of unreinforced soil

The load-settlement curves for unreinforced sands under loading with different eccentricities are displayed in Fig. 6. For each load eccentricity value, the oil percentage contents were 3, 6, 9, and 12%. As can be observed, the oil in the soil led to diminishes the bearing capacity under all

eccentricity values. The load-settlement curves of oil-contaminated soil failed at lower settlement values compared to unreinforced soil for both loadings applied along the centerline of the footing and also with different eccentricities. Further, the settlement value declined with an increase in oil content. The bearing capacity of unreinforced sand models for s/B ratios of 2.5, 5, and 10% and different oil contents are presented in Table 4. As can be seen, the rate of load capacity reduction increases with increasing load eccentricity and settlement value. For instance, for e/B ratios of 0, 1/12, 1/6, and 1/3 containing 3% oil, the bearing capacity for the settlement value of s/B=2.5% compared to clean sand decreased by about 6.9, 7.2, 7.47, and 9.44%, respectively, and for s/B=5%, it reduced by about 10.43, 10.57, 11.52, and 15.50%, respectively.

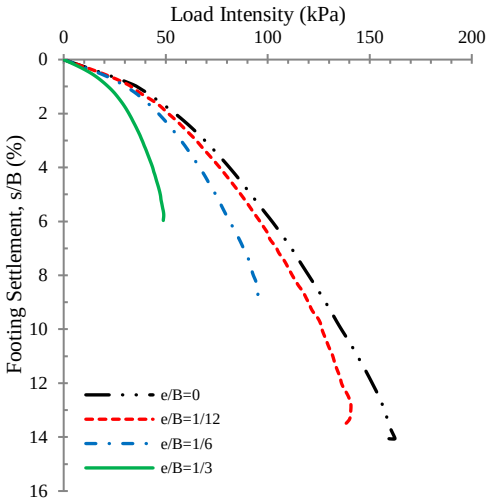

Fig. 5. Load-settlement curves for unreinforced sand model under different eccentricity values

Table 3. Load eccentricity effect on bearing capacity of strip footing located on the clean sand

e/B	Bearing capacity of footing at different settlement (kPa)						q_{ult} (kPa)	q_{ult} reduction (%)
	s/B=2.5%	R (%)	s/B=5%	R (%)	s/B=10%	R (%)		
0	62.27	0	92.67	0	136.00	0	162.31	0
1/12	58.57	6	87.45	6	126.60	7	140.79	13
1/6	52.20	16	74.60	19	-	-	95.33	41
1/3	35.27	43	47.34	49	-	-	49.03	70

Note: R=reduction magnitude of bearing capacity
- : the model is failed

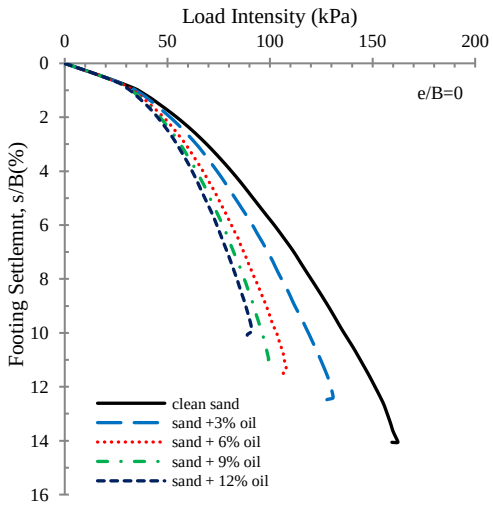

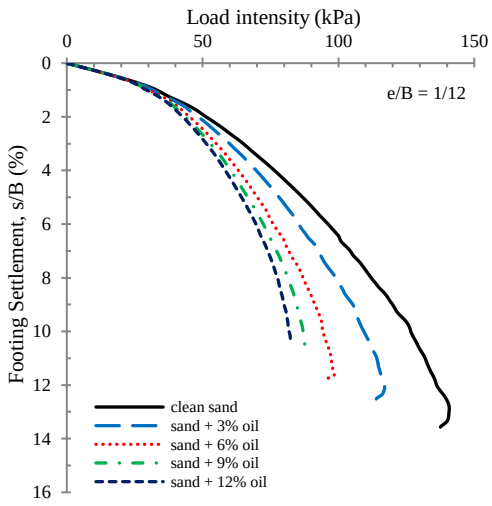

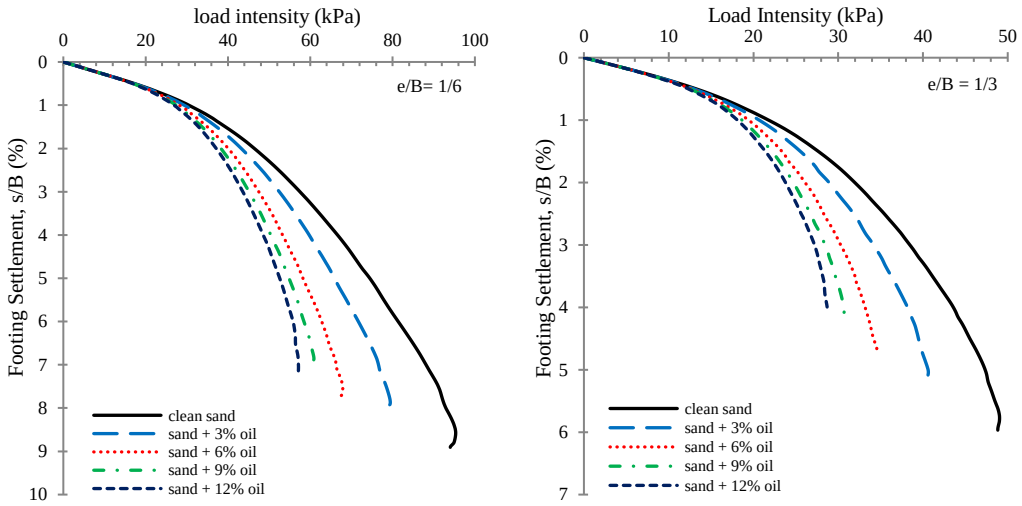

Fig. 6. Load-settlement curves of the footing on the contaminated sand under different eccentricity values

Table 4. Bearing capacity of strip footing on the contaminated unreinforced sand under different eccentricities

Load Eccentricity (e/B)	Percentages of oil pollution	Bearing capacity (kPa)		
		s/B=2.5%	s/B=5%	s/B=10%
0	Clean sand	62.27	92.67	136.00
	Sand + 3% oil	57.97	83.00	119.00
	Sand + 6% oil	53.99	74.60	103.52
	Sand + 9% oil	51.73	70.84	96.19
	Sand + 12% oil	50.27	68.49	90.15
1/12	Clean sand	58.57	87.45	126.60
	Sand + 3% oil	54.35	78.20	109.50
	Sand + 6% oil	50.50	70.20	94.32
	Sand + 9% oil	48.66	66.83	87.00
	Sand + 12% oil	47.00	64.50	81.88
1/6	Clean sand	52.20	74.60	-
	Sand + 3% oil	48.30	66.00	-
	Sand + 6% oil	44.70	58.43	-
	Sand + 9% oil	42.48	55.00	-
	Sand + 12% oil	40.74	52.59	-
1/3	Clean sand	35.27	47.34	-
	Sand + 3% oil	31.94	40.61	-
	Sand + 6% oil	28.28	-	-
	Sand + 9% oil	26.72	-	-
	Sand + 12% oil	25.64	-	-

The reduction rate of carrying capacity for loading applied along and outside of the footing's centerline decreased with increasing oil content. For instance, the bearing capacity of footing for e/B=0 by increasing oil content from 0 to 3, 3 to 6, 6 to 9, and 9 to 12% in the settlement value of s/B=2.5% reduced by about 6.9, 6.86, 4.18, and 2.82%, respectively, and for s/B=10% it decreased by about 12.50, 12.16, 7.97, and 6.27%, respectively. The reduction for e/B=1/6 under similar oil contents in s/B=2.5% was about 7.47, 7.45, 4.97, and 4.09%, but it was failed under s/B=10%.

5.3 The effect of reinforcement on the load-settlement of the footing located on oil-contaminated sand

The effect of geocell-reinforcement on load-settlement curves for footing located on contaminated sand with different oil percentages of 3 and 12% under different loading eccentricity

values is shown in Fig. 7. In this case, the ratio of the height and width of the geocell to the width of the footing is considered h/B=0.45 and b/B=4, respectively. For all these tests, the ratio of reinforcement depth to the width of the footing is u/B=0.1.

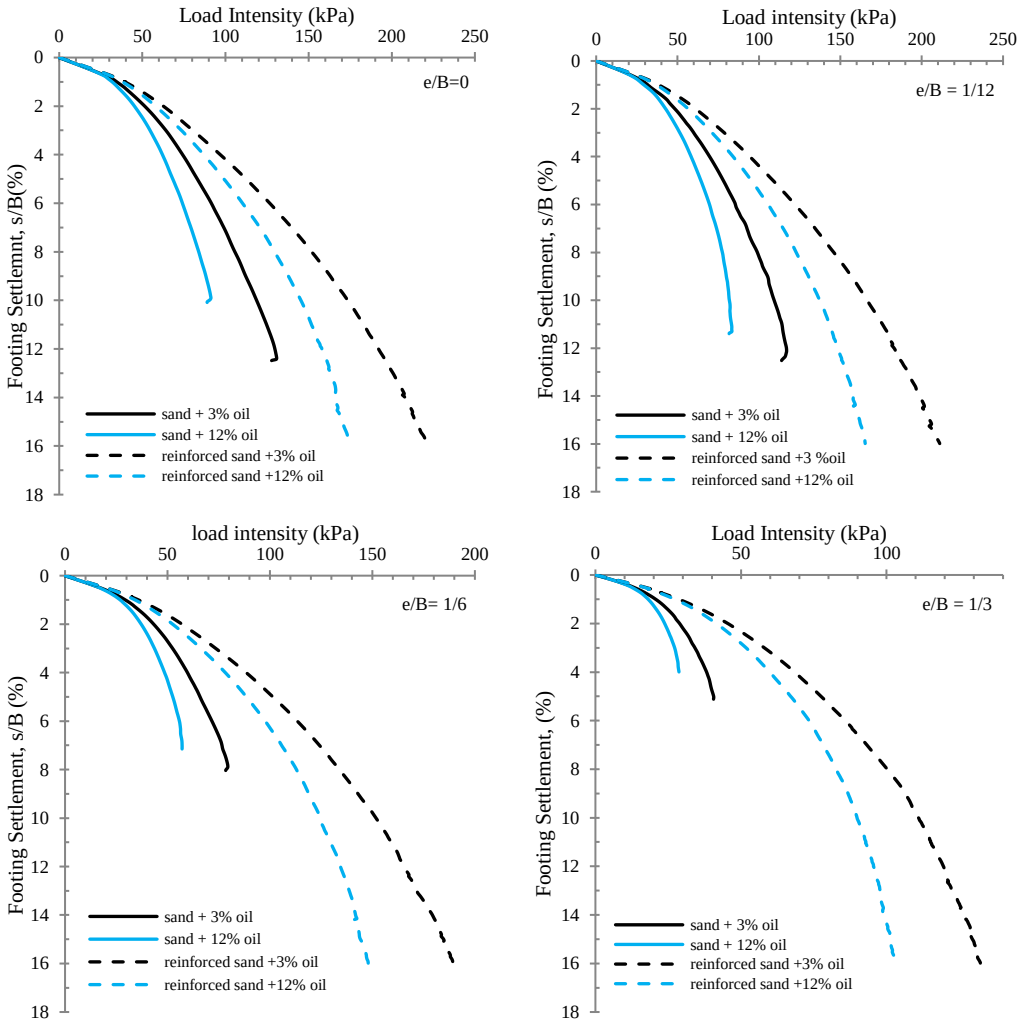

Fig. 7. Load-settlement curves for unreinforced and reinforced sand with different oil contents under different eccentricity values

It can be seen that geocell-reinforcement increases the bearing capacity of the footing located on the oil-contaminated soil under loading with different eccentricities. The ultimate bearing capacity of unreinforced footings can be determined with 3 and 12% oil contents for loadings along and outside of the footing's centerline. However, it cannot be determined for geocell-reinforced soil with 3 and 12% oil contents. The results reported by Jahanian et al. [50] for geocell-reinforced footings laid on clean sand revealed that the ultimate bearing capacity cannot determined for low eccentricity values such as e/B=1/12, even for settlements that are about 50% of the footing's width. However, it occurred at higher settlements for higher eccentricities with ratios of e/B=1/6, 1/3, almost three times that of unreinforced sand models.

The changes in the bearing capacity improvement factor (IF) obtained from the results of the tests conducted for footings located on reinforced sand contaminated with different oil contents are depicted in Fig. 8. As can be seen, the effect of geocell on polluted soil was greater than its effect

on clean soil. Further, the improvement coefficient of the carrying capacity increased with increasing oil content and settlement magnitude. IF values for s/B=2.5% and oil contents of 0, 3, 6, 9, and 12% under e/B=1/6 eccentricity were 1.32, 1.35, 1.41, 1.44, and 1.47, respectively. However, IF values for s/B=10% under the same values of oil content and eccentricity were obtained by about 1.77, 1.91, 2.00, 2.11, and 2.17, respectively. From Fig. 8 it can be observed that the reinforcing effect has increased with an increase in loading eccentricity for both clean and contaminated soils. For instance, the increased magnitude for clean sand under loading with loading eccentricities of 0, 1/12, 1/6, and 1/3 for s/B=10% was about 1.42, 1.46, 1.77, and 2.53, respectively. The IF values for similar e/B and s/B for contaminated soil containing 12% oil were obtained by about 1.61, 1.67, 2.17, and 3.13, respectively. It was observed that using geocell had the greatest effect when the loading was exerted outside the foundation's core, i.e., e/B>1/6. Previous studies also showed that the strengthening effect was more eminent for higher eccentricity values [37, 50, 54].

Soil displacement beneath the foundation for unreinforced contaminated soil with 12% oil content under loading exerted along the footing's centerline and also with different eccentricities of e/B=1/12, 1/6, 1/3 by keeping the same scale in horizontal and vertical directions is depicted in Fig. 9. As can be observed, displacement contours for e/B=0 is symmetrical. However, eccentric loading has caused the asymmetry of the soil displacement. The main reason for this issue is the footing tilting around the centerline axis. In addition, it can be discerned that the displacement depth is reduced by increasing load eccentricity. This issue can be attributed to the depth of the stress-affected zone, which decreases with increasing eccentricity.

The effect of presenting a geocell beneath the footing for contaminated soil with 12% oil under e/B=0 and e/B=1/6 is also provided in Figs. 10a and 10b. It can be seen that displacement depth beneath the footing under e/B=1/6 eccentricity was lower compared to loading applied along the footing's centerline. By comparing Figs. 9 and Figs. 10 it can be discerned that the non-symmetrical failure pattern in this condition is not extended such as unreinforced cases. As can be observed, displacement depth for geocell-reinforced cases was much deeper than the unreinforced soil models under similar eccentric loading values. Further, the geocell plays an essential role in increasing the load capacity since it distributes stress to a deeper layer of the soil, causing a larger area of the soil medium affected by the stress field, which enhances the ultimate bearing capacity of the footing.

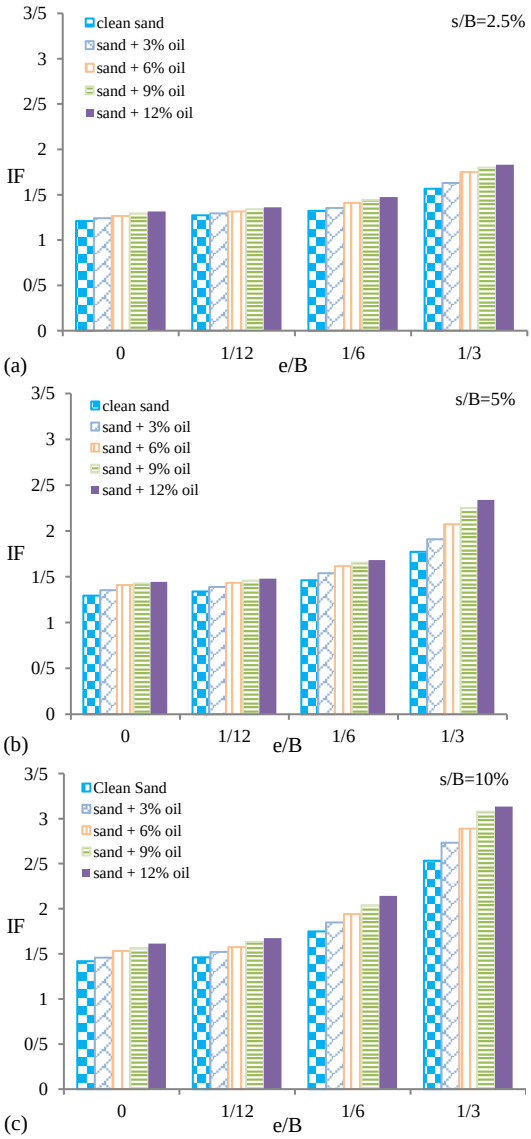

Fig. 8. Improvement factor of bearing capacity against eccentricity for various oil contents under different settlement values of (a) s/B=2.5%, (b) s/B=5%, (c) s/B=10%

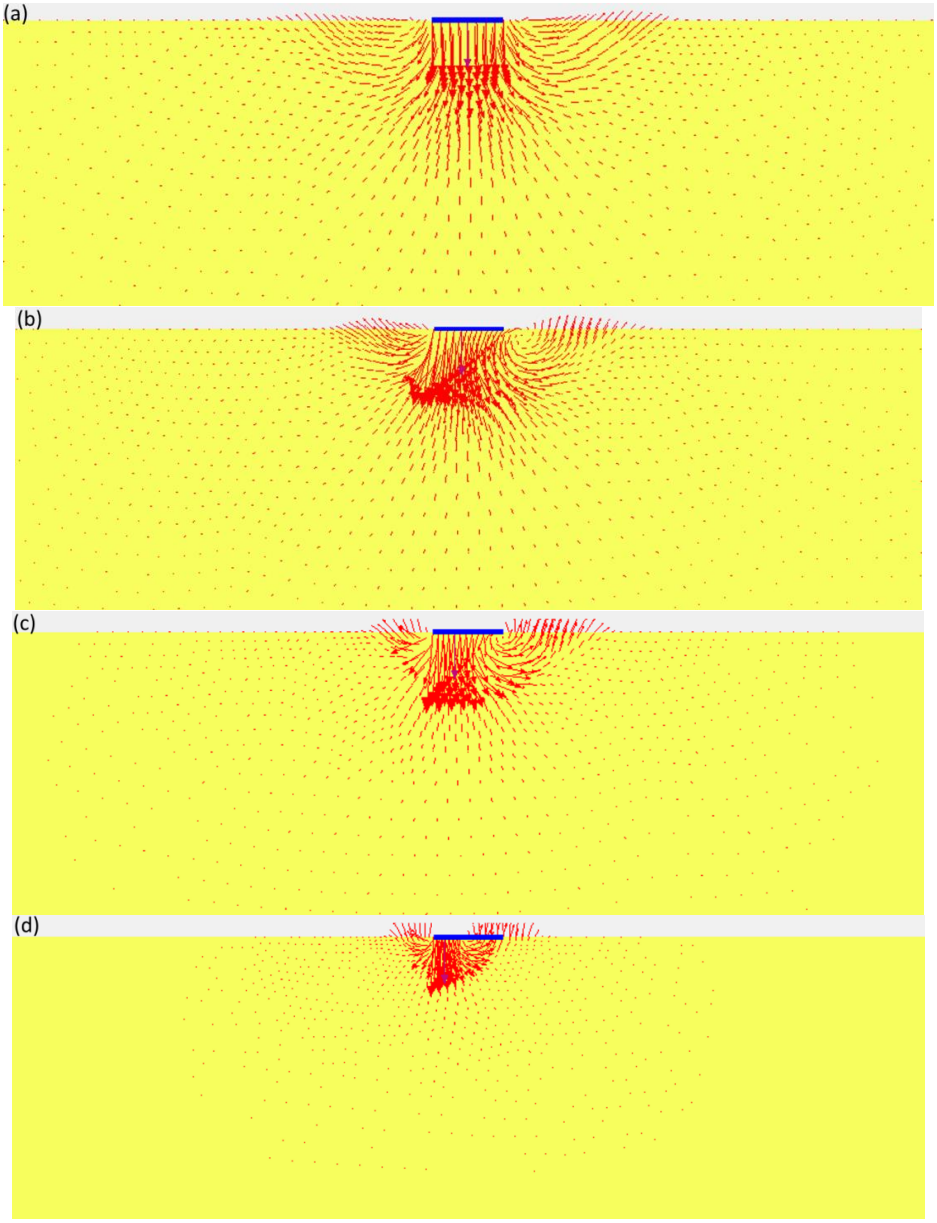

Fig. 9. Displacement contour beneath the footing for unreinforced contaminated soil under loading with different eccentricities, (a) e/B=0, (b) e/B=1/12, (c) e/B=1/6, (d) e/B=1/3

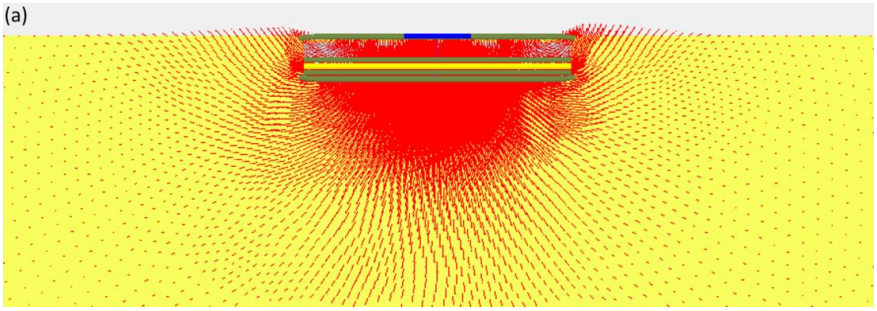

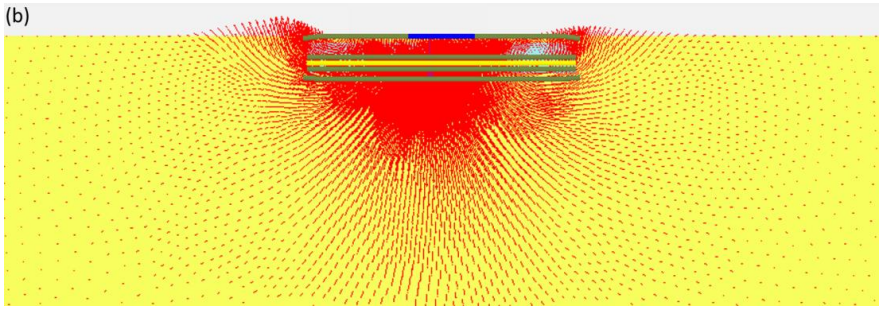

Fig. 10. Displacement contour beneath the footing for geocell-reinforced contaminated soil under loading with eccentricities of (a) e/B=0, (b) e/B=1/6

6. Conclusion

In this research, the behavior of strip footings located on geocell-reinforced sand with and without oil pollution under eccentric loading was evaluated using numerical modeling. The results were compared with those obtained from laboratory tests. The main findings of the study can be summarized as follows:

- The presence of oil in the unreinforced soil led to a reduction in the bearing capacity for all loading eccentricities.
- The ultimate bearing capacity of unreinforced sand decreased dramatically with an increase in load eccentricity, and the reduction rate was significantly increased for e/B>1/6.
- The load-settlement curves of unreinforced soil contaminated with oil for both loadings along and outside of the footing centerline failed at lower settlements compared to clean soil, and the settlement value decreased with an increase in oil content. The reduction rate of the carrying capacity decreased with the increase in oil content for all loading conditions and increased with increasing load eccentricity and settlement value.
- Reinforcement of soil with geocell resulted in increased load capacity of foundations located in oil-contaminated soil under all eccentricity values.
- The ultimate bearing capacity of unreinforced models for clean and contaminated sands with different oil contents can be determined under different loading eccentricities; however, it cannot be determined for footings located on reinforced sand.
- The effect of reinforcement with geocell for polluted soil was higher than that of clean soil. The bearing capacity improvement factor increased with increasing oil content and settlement value. The reinforcing effect increased with increasing load eccentricity for both clean and contaminated soils. Using geocells for loading applied outside the foundation core, i.e., e/B>1/6, had the most positive effect.
- The footing tilting around the centerline axis of the footing due to load eccentricity as well as soil reinforcement with geocell led to a reduction in the stress-affected zone and as a result the displacement depth of the soil beneath the foundation.

Declaration of Competing Interest

The authors declare that they have no known competing financial interests or personal relationships that could have appeared to influence the work reported in this paper.

7. References

[1] Ahmadi, S., Kamalian, M., and Askari, F. (2021). Evaluation of the static bearing capacity coefficients of rough strip footing using the stress characteristics method. *Int. J. Civ. Eng*. 19(2): 155–165. https://doi.org/10.1007/s40999-020-00539-y.

[2] Ahmadi, S., Kamalian, M., and Askari, F. (2020). Considerations on Bearing Capacity Factors of Rough Strip Footing Using the Stress Characteristics Method. *Iran. J. Sci. Technol. Trans. Civ. Eng*. 45(4): 2611–2621. https://doi.org/10.1007/s40996-020-00495-6.

[3] Khosravi, E., Ghasemzadeh, H., Sabour, M.R., Yazdani, H. (2013). Geotechnical properties of gas oil-contaminated kaolinite. Engineering Geology, 166, 11–16. https://doi.org/10.1016/j.enggeo.2013.08.004.

[4] Ahmadi, M., Ebadi, T. and Maknoon, R., (2021). Effects of crude oil contamination on geotechnical properties of sand-kaolinite mixtures. Engineering geology, 283, p.106021. https://doi.org/10.1016/j.enggeo.2021.106021.

[5] Nasehi, S.A., Uromeihy, A., Nikudel, M.R. and Morsali, A., (2016). Influence of gas oil contamination on geotechnical properties of fine and coarse-grained

soils. Geotechnical and Geological Engineering, 34, pp.333-345. https://doi.org/10.1007/s10706-015-9948-7.
[6] Safehian, H., Rajabi, A.M. and Ghasemzadeh, H., (2018). Effect of diesel-contamination on geotechnical properties of illite soil. engineering geology, 241, pp.55-63. https://doi.org/10.1016/j.enggeo.2018.04.020.
[7] Chen, Q., He, Y. and Zhang, Z., (2022). Effects of diesel contamination on geotechnical properties of granitic residual soil. Arabian Journal of Geosciences, 15(17), p.1474. https://doi.org/10.1007/s12517-022-10756-5.
[8] Ghasemzadeh, H., Tabaiyan, M. (2017). The Effect of Diesel Fuel Pollution on the Efficiency of Soil stabilization Method. Geotechnical and Geological Engineering, 35, 475–484. https://doi.org/10.1007/s10706-016-0121-8.
[9] Khamehchiyan, M., Charkhabi, A.H. and Tajik, M., (2007). Effects of crude oil contamination on geotechnical properties of clayey and sandy soils. Engineering geology, 89(3-4), pp.220-229. https://doi.org/10.1016/j.enggeo.2006.10.009.
[10] Karkush, M.O. and Kareem, Z.A., (2017). Investigation of the impacts of fuel oil on the geotechnical properties of cohesive soil. Engineering Journal, 21(4), pp.127-137. https://doi.org/10.4186/ej.2017.21.4.127.
[11] Nasr, A.M., (2009). Experimental and theoretical studies for the behavior of strip footing on oil-contaminated sand. Journal of geotechnical and geoenvironmental engineering, 135(12), pp.1814-1822. https://doi.org/10.1061/(ASCE)GT.1943-5606.0000165.
[12] Hosseini, A. and Hajiani Boushehrian, A., (2019). Laboratory and numerical study of the behavior of circular footing resting on sandy soils contaminated with oil under cyclic loading. Scientia Iranica, 26(6), pp.3219-3232. DOI: 10.24200/SCI.2018.5427.1267.
[13] Joukar, A. and Boushehrian, A.H., (2020). Experimental study of strip footings rested on kerosene oil-and gas oil-contaminated sand slopes. Iranian Journal of Science and Technology, Transactions of Civil Engineering, 44, pp.209-217. https://doi.org/10.1007/s40996-018-00231-1.
[14] Al-Adly, A.I.F., Fadhil, A.I. and Fattah, M.Y., (2019). Bearing capacity of isolated square footing resting on contaminated sandy soil with crude oil. Egyptian Journal of Petroleum, 28(3), pp.281-288. https://doi.org/10.1016/j.ejpe.2019.06.005.
[15] Shin, E.C., Lee, J.B. and Das, B.M., (1999). Bearing capacity of a model scale footing on crude oil-contaminated sand. Geotechnical & Geological Engineering, 17, pp.123-132. https://doi.org/10.1023/A:1016078420298.
[16] Nasr, A.M., (2016). Behaviour of strip footing on oil-contaminated sand slope. International Journal of Physical Modelling in Geotechnics, 16(3), pp.134-151. https://doi.org/10.1680/jphmg.15.00014.
[17] Dash, S.K., Krishnaswamy, N.R. and Rajagopal, K., (2001). Bearing capacity of strip footings supported on geocell-reinforced sand. Geotextiles and Geomembranes, 19(4), pp.235-256. https://doi.org/10.1016/S0266-1144(01)00006-1.
[18] Sitharam, T.G. and Sireesh, S., (2006). Effects of base geogrid on geocell-reinforced foundation beds. Geomechanics and Geoengineering: An International Journal, 1(3), pp.207-216. https://doi.org/10.1080/17486020600900596.
[19] Thallak, S.G., Saride, S., Dash, S.K. (2007). Performance of surface footing on geocell-reinforced soft clay beds. Geotechnical and Geological Engineering, 25, 509–524. https://doi.org/10.1007/s10706-007-9125-8.
[20] Zhou, H., Wen, X. (2008). Model studies on geogrid- or geocell-reinforced sand cushion on soft soil. Geotextiles and Geomembranes, 26, 231–238. https://doi.org/10.1016/j.geotexmem.2007.10.002.
[21] Pokharel, S.K., Han, J., Parsons, R.L., Qian, Y., Leshchinsky, D. and Halahmi, I., (2009). Experimental study on bearing capacity of geocell-reinforced bases. In 8th international conference on Bearing Capacity of Roads, Railways and Airfields (pp. 1159-1166). June 2009: Champaign, IL, USA.
[22] Sireesh, S., Sitharam, T.G. and Dash, S.K., (2009). Bearing capacity of circular footing on geocell–sand mattress overlying clay bed with void. Geotextiles and Geomembranes, 27(2), pp.89-98. https://doi.org/10.1016/j.geotexmem.2008.09.005.
[23] Tafreshi, S.M. and Dawson, A.R., (2010). Comparison of bearing capacity of a strip footing on sand with geocell and with planar forms of geotextile reinforcement. Geotextiles and Geomembranes, 28(1), pp.72-84. https://doi.org/10.1016/j.geotexmem.2009.09.003.
[24] Yang, X., Han, J., Pokharel, S.K., Manandhar, C., Parsons, R.L., Leshchinsky, D. and Halahmi, I., (2012). Accelerated pavement testing of unpaved roads with geocell-reinforced sand bases. Geotextiles and Geomembranes, 32, pp.95-103. https://doi.org/10.1016/j.geotexmem.2011.10.004.
[25] Fazeli Dehkordi, P., Ghazavi, M., Ganjian, N. and Karim, U.F.A., (2019). Effect of geocell-reinforced sand base on bearing capacity of twin circular footings. Geosynthetics International, 26(3), pp.224-236. https://doi.org/10.1680/jgein.19.00047.
[26] Changizi, F., Razmkhah, A., Ghasemzadeh, H. and Amelsakhi, M., (2022). Behavior of geocell-reinforced soil abutment wall: A physical modeling. Journal of Materials in Civil Engineering, 34(3), p.04021495. https://doi.org/10.1061/(ASCE)MT.1943-5533.0004132.
[27] Madhavi Latha, M., Somwanshi, A. (2009). Effect of reinforcement form on the bearing capacity of square footings on sand. Geotextiles and Geomembranes, 27, 409–422. https://doi.org/10.1016/j.geotexmem.2009.03.005.
[28] Dash, S.K., Rajagopal, K. and Krishnaswamy,

N.R., (2001). Strip footing on geocell reinforced sand beds with additional planar reinforcement. Geotextiles and Geomembranes, 19(8), pp.529-538. https://doi.org/10.1016/S0266-1144(01)00022-X.
[29] Dash, S.K., Reddy, P.D.T. and Raghukanth, S.T.G., (2008). Subgrade modulus of geocell-reinforced sand foundations. Proceedings of the Institution of Civil Engineers-Ground Improvement, 161(2), pp.79-87. https://doi.org/10.1680/grim.2008.161.2.79.
[30] Dash, S.K., (2012). Effect of geocell type on load-carrying mechanisms of geocell-reinforced sand foundations. International Journal of Geomechanics, 12(5), pp.537-548. https://doi.org/10.1061/(ASCE)GM.1943-5622.0000162.
[31] Mehrjardi, G.T. and Motarjemi, F., (2018). Interfacial properties of Geocell-reinforced granular soils. Geotextiles and Geomembranes, 46(4), pp.384-395. https://doi.org/10.1016/j.geotexmem.2018.03.002.
[32] Mehrjardi, G.T., Behrad, R. and Tafreshi, S.M., (2019). Scale effect on the behavior of geocell-reinforced soil. Geotextiles and Geomembranes, 47(2), pp.154-163. https://doi.org/10.1016/j.geotexmem.2018.12.003.
[33] Pokharel, S.K., Han, J., Leshchinsky, D., Parsons, R.L., Halahmi, I. (2010). Investigation of factors influencing behavior of single geocell-reinforced bases under static loading. Geotextiles and Geomembranes 28, 570-578. http://doi.org/10.1016/j.geotexmem.2010.06.002.
[34] Patra, C.R., Das, B.M. and Atalar, C., (2005). Bearing capacity of embedded strip foundation on geogrid-reinforced sand. Geotextiles and Geomembranes, 23(5), pp.454-462. https://doi.org/10.1016/j.geotexmem.2005.02.001.
[35] El Sawwaf, M.A., (2007). Behavior of strip footing on geogrid-reinforced sand over a soft clay slope. *Geotextiles and Geomembranes*, 25(1), 50-60. https://doi.org/10.1016/j.geotexmem.2006.06.001.
[36] El Sawwaf, M., (2009). Experimental and numerical study of eccentrically loaded strip footings resting on reinforced sand. Journal of Geotechnical and Geoenvironmental Engineering, 135(10), pp.1509-1518. https://doi.org/10.1061/(ASCE)GT.1943-5606.0000093.
[37] El Sawwaf, M. and Nazir, A., (2012). Behavior of eccentrically loaded small-scale ring footings resting on reinforced layered soil. *Journal of Geotechnical and Geoenvironmental Engineering*, 138(3), 376-384. https://doi.org/10.1061/(ASCE)GT.1943-5606.0000593.
[38] Badakhshan, E. and Noorzad, A., (2015). Load eccentricity effects on behavior of circular footings reinforced with geogrid sheets. Journal of Rock Mechanics and Geotechnical Engineering, 7(6), pp.691-699. https://doi.org/10.1016/j.jrmge.2015.08.006.
[39] Dash, S.K., (2010). Influence of relative density of soil on performance of geocell-reinforced sand foundations. Journal of Materials in Civil Engineering, 22(5), pp.533-538. https://doi.org/10.1061/(ASCE)MT.1943-5533.0000040.
[40] Moghaddas Tafreshi, S.N., Sharifi, P., Dawson, A.R. (2016). Performance of circular footings on sand by use of multiple-geocell or –planar geotextile reinforcing layers. Soils and Foundations, 56(6), 984–997: http://doi.org/10.1016/j.sandf.2016.11.004.
[41] Shadmand, A., Ghazavi, M. and Ganjian, N., (2018). Load-settlement characteristics of large-scale square footing on sand reinforced with opening geocell reinforcement. *Geotextiles and Geomembranes*, 46(3), 319-326. https://doi.org/10.1016/j.geotexmem.2018.01.001.
[42] Mehdipour, I., Ghazavi, M., Moayed, R.Z. (2013). Numerical study on stability analysis of geocell reinforced slopes by considering the bending effect. Geotextiles and Geomembranes, 37, 23–34. https://doi.org/10.1016/j.geotexmem.2013.01.001.
[43] Hegde, A., Sitharam, T.G. (2013). Experimental and numerical studies on footings supported on geocell reinforced sand and clay beds. International Journal of Geotechnical Engineering, 7(4), 346–354. https://doi.org/10.1179/1938636213Z.00000000043.
[44] Changizi, F., Razmkhah, A., Ghasemzadeh, H. and Amelsakhi, M., (2021). Effect of oil-contamination on behavior of geocell-reinforced soil abutment wall. Journal of Petroleum Geomechanics; Vol, 4(1). DOI: 10.22107/jpg.2022.333533.1161.
[45] Hegde, A.M, Sitharam, T.G. (2015). Three-dimensional numerical analysis of geocell-reinforced soft clay beds by considering the actual geometry of geocell pockets. Canadian Geotechnical Journal, 52, 1–12. https://doi.org/10.1139/cgj-2014-0387.
[46] Chowdhury, S. and Patra, N.R., (2021). Settlement behavior of circular footing on geocell-and geogrid-reinforced pond ash bed under combine static and cyclic loading. Arabian Journal of Geosciences, 14(11), p.1063. https://doi.org/10.1007/s12517-021-07424-5.
[47] Bathurst, R.J., Karpurapu, R.G. (1993). Large-scale triaxial compression testing of geocell-reinforced granular soils. Geotechnical Testing Journal, 16, 296–303. http://doi.org/10.1520/GTJ10050J.
[48] Rajagopal, K., Krishnaswamy, N.R., and Madhavi Latha, G. (1999). Behavior of sand confined in single and multiple geocells. Geotextiles and Geomembranes, 17, 171–184. https://doi.org/10.1016/S02661144(98)00034-X.
[49] Madhavi Latha, M., Rajagopal, K. (2007). Parametric finite element analyses of geocell-supported embankments. Canadian Geotechnical Journal, 44, 917–927. https://doi.org/10.1139/T07-039.
[50] Jahanian, M. S., Razmkhah, A., Ghasemzadeh, H., & Vosoughifar, H. (2022). Bearing capacity of the strip footing located on the sand reinforced by geocell under eccentric load. *Arabian Journal of*

Geosciences, *15*(15), 1328. https://doi.org/10.1007/s12517-022-10600-w.
[51] Madhavi Latha, G., (2000). Investigations on the behaviour of geocell supported embankments. *PhD.* thesis, Department of Civil Engineering, *Indian Institute of Technology, Madras, Chennai*.
[52] Soltani-Jigheh, H., Vafaei Molamahmood, H., Ebadi, T., Soorki, A.A. (2018). Effect of Oil-Degrading Bacteria on Geotechnical Properties of Crude Oil–Contaminated Sand. Environmental & Engineering Geoscience, 24 (3), 333–341. https://doi.org/10.2113/EEG-1883.
[53] Badakhshan, E. and Noorzad, A., (2017). Effect of footing shape and load eccentricity on behavior of geosynthetic reinforced sand bed. *Geotextiles and Geomembranes*, 45(2), 58-67. https://doi.org/10.1016/j.geotexmem.2016.11.007.
[54] Gill, G. and Mittal, R.K., (2019). Use of waste tire-chips in shallow footings subjected to eccentric loading-an experimental study. Construction and Building Materials, 199, pp.335-348. https://doi.org/10.1016/j.conbuildmat.2018.12.024.